ELECTRONIC SUPPLEMENTARY INFORMATION FOR THE MANUSCRIPT

Strain engineering of photo-induced phase transformations in Prussian blue analogue heterostructures

Adeline Adam, Mélanie Poggi, Eric Larquet, Robert Cortès, Lucio Martinelli, Pierre-Eugène Coulon, Eric Lahera, Olivier Proux, Dmitry Chernyshov, Kamel Boukheddaden, Thierry Gacoin and Isabelle Maurin

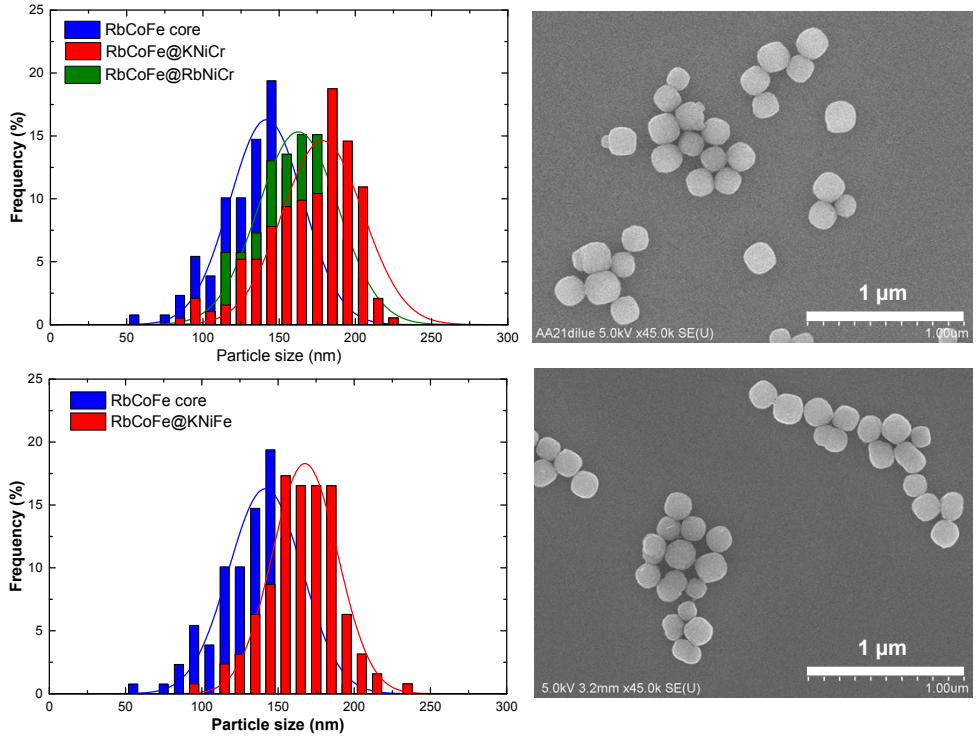

Fig. S1 Histograms showing the distribution of particle sizes for the core-shell samples and the bare core particles, determined by SEM using the ImageJ software (http://rsbweb.nih.gov/ij/). Statistics were performed over more than 200 particles for each sample. A 10 nm bin size was used for the histograms and the curves were fit to Gaussian functions. Representative SEM images are shown on the right side for RbCoFe@KNiCr (**2**) and RbCoFe@KNiFe (**3**) particles. The preparation of the samples for SEM observations is detailed in Presle *et al.*, *New J. Chem.*, 2011, **35**, 1296.

The overall composition of the core-shell particles was obtained by x-ray Energy Dispersive Spectroscopy and the chemical formula of the shell was derived assuming that there is no intermixing between the core and shell components.

Table S1 Chemical characterization of the bare core and core-shell samples by EDS

	Fe/Co(core)	Rb/Co(core)	Cr/Ni(shell)	K(Rb)/Ni(shell)[a]	Ni(shell)/Co(core)
RbCoFe (**1**)	0.80(2)	0.46(3)			
RbCoFe@KNiCr (**2**)	0.79(2)		0.69(5)	0.1(1)	0.84(5)
KNiCr	-		0.71(2)	0.12(6)	-
RbCoFe@RbNiCr	0.80(1)		0.71(2)	0.13(6)	0.86(2)
RbNiCr	-		0.73(1)	0.18(3)	-
	Fe/Co (core)		**Fe/Ni (shell)**	**K/Ni (shell)**	**Ni(shell)/Co(core)**
RbCoFe@KNiFe (**3**)	0.80(2)[b]		0.8(1)	0.5(3)	0.80(3)
KNiFe			0.73(2)	0.18(6)	

[a] from electroneutrality, [b] value measured for the bare cores.

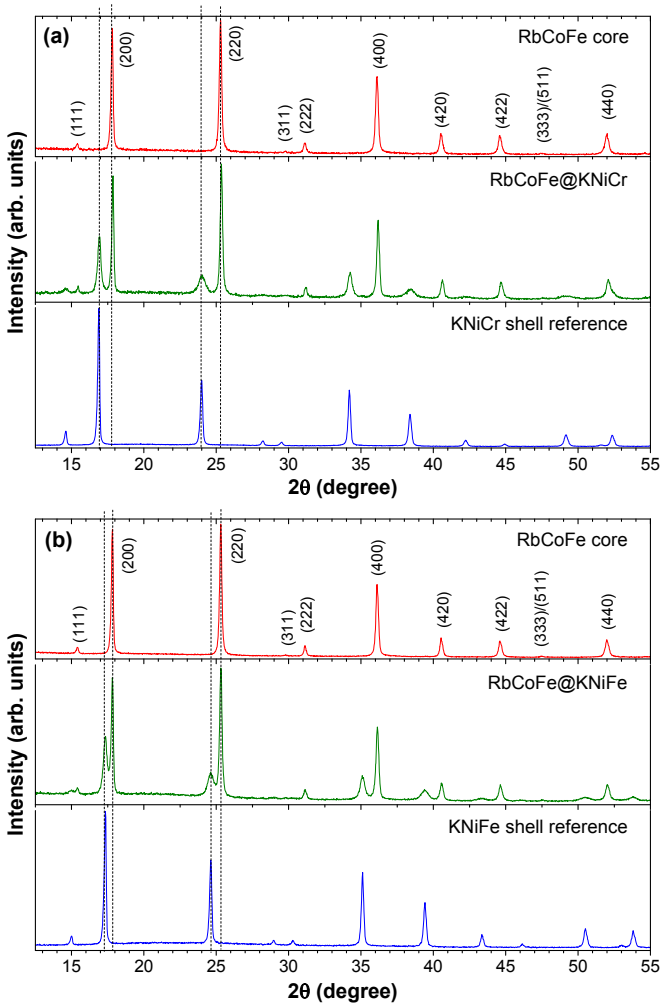

Fig. S2 Room temperature PXRD patterns of the two core-shell samples, compared to those of the RbCoFe primary particles and of the KNiCr (a) and KNiFe (b) reference compounds (λ = 1.5418 Å).

Chemical mapping by EDS.

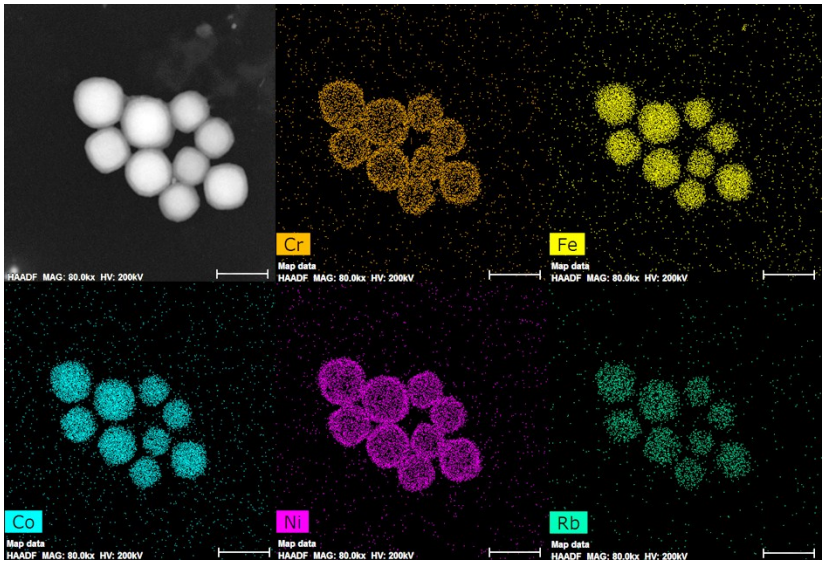

Fig. S3 STEM-HAADF image and chemical mapping of RbCoFe@KNiCr particles (sample **2**), scale bar: 200 nm. The following peaks were monitored by EDS: Cr (Kα) 5,411 eV, Fe (Kα) 6,398 eV, Co (Kα) 6,924 eV, Ni (Kα) 7,471 eV and Rb (Kα) 13,373 eV.

Williamson-Hall analyses.

$$\frac{H_{hkl}\cos\theta}{\lambda} = \frac{1}{L_{hkl}} + \varepsilon_{hkl}\frac{2\sin\theta}{\lambda} \qquad (1)$$

Equation (1) is based on lorentzian line shapes. H_{hkl} refers to the Full Width at Half Maximum (FWHM) corrected for the instrumental resolution function of a given (*hkl*) Bragg reflection, 2θ is the angle of diffraction and λ denotes the x-ray wavelength. L_{hkl} and ε_{hkl} values are experimentally determined from linear regressions to Equation 1. We actually made several approximations (use of FWHM rather than integral breadth values, use of a Cauchy approximation while we fitted the experimental linewidths with Pseudo-Voigt functions and typical mixing parameters of 0.75). As coherence length values are sensitive to these approximations, we restricted our analyses to qualitative comparisons of the microstrain parameters in the different samples.

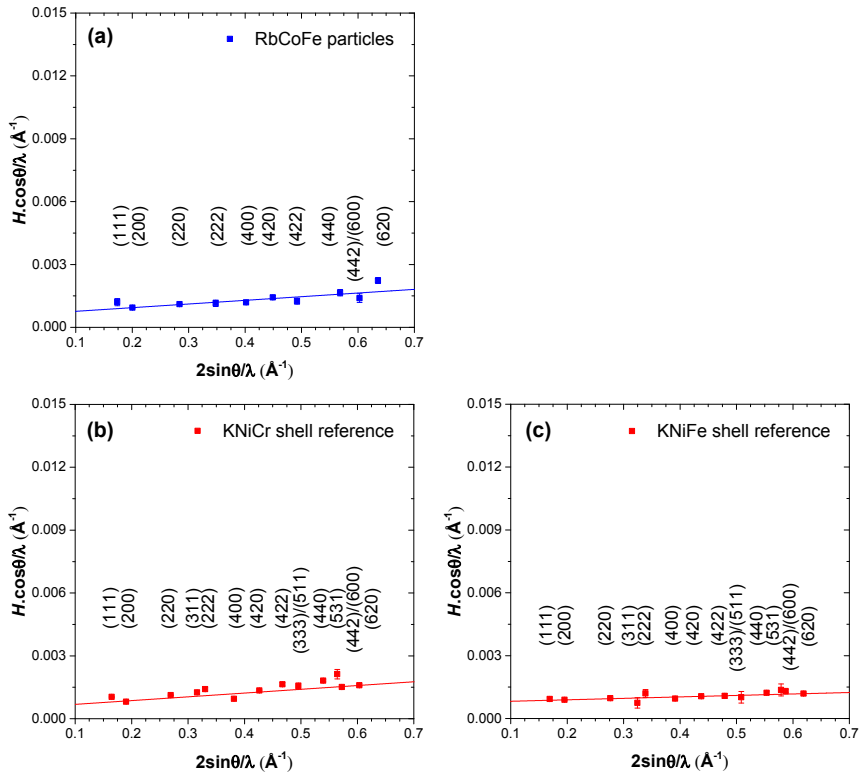

Fig. S4 Williamson-Hall plots for the bare RbCoFe primary particles (a) and for the single-phase compounds KNiCr (b) and KNiFe (c).

Complementary characterizations for the RbCoFe@RbNiCr core-shell sample.

Table S2 Structural parameters derived from the PXRD data at ambient temperature

	mean core size / standard deviation (nm)	shell thickness (nm)	atomic ratio Ni/Co	*a* core (Å)	ε_{hkl} core (%)	*a* shell (Å)	ε_{hkl} shell (%)	ε_{h00} shell (%)
RbCoFe	141 / 22			9.943(5)	0.20(3)	-	-	-
RbCoFe@RbNiCr	162 / 25	10.5	0.86(2)	9.934(5)	0.26(4)	10.485(5)	1.4(4)	0.32
RbNiCr	134 / 32	-		-	-	10.475(5)	0.19(3)	

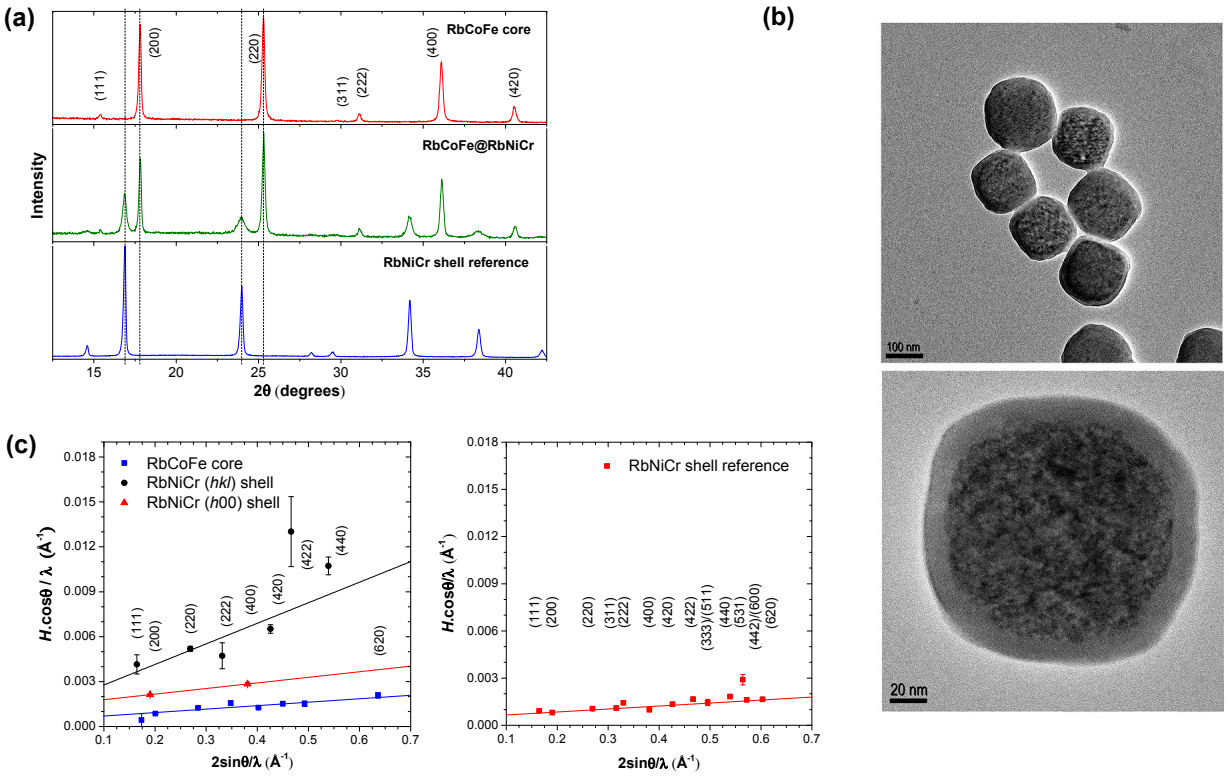

Fig. S5 (a) Room temperature PXRD patterns of the RbCoFe@RbNiCr heterostructure, RbCoFe primary particles and RbNiCr standard (λ= 1.5418 Å); (b) Bright-field TEM images of the core-shell particles; (c) Williamson-Hall plots derived from these PXRD profiles for the RbCoFe@RbNiCr sample and RbNiCr reference.

Synthesis of the RbCoFe, KNiCr and KNiFe samples used for optical characterizations.

200 mL of an aqueous solution of $NiCl_2$ (1 mM) were rapidly poured into a solution of $K_3Cr(CN)_6$ [or $K_3Fe(CN)_6$] (200 mL, 1 mM) placed under vigorous stirring (800 rpm). Half of the solution was kept for optical characterizations. The other half was centrifuged a first time at 60,000 g for 30 min and washed three times with water using again centrifugation at 60,000 g. A light blue-green powder was recovered for KNiCr and dark yellow for KNiFe. Another RbCoFe colloid, with ~ 20 nm hydrodynamic diameter, was also prepared based on the first synthesis step involved in the growth of the 140 nm core particles, using again rapid pouring instead of slow addition.

The UV-vis absorption spectra of the RbCoFe, KNiCr and KNiFe colloids were recorded with a Cary 50 spectrometer. The supernatant of the first centrifugation at 60,000 g was used as a reference to subtract the contributions from unreacted species (e.g., $[Fe(CN)_6]^{3-}$ and $[Cr(CN)_6]^{3-}$ excess ions). The colloid concentrations were estimated by weighing the powder recovered after drying 20 mL of the post-synthesis solutions. Note that the synthesis procedures were modified with respect to those described in the main text in order to get smaller particles and limit the effect of light scattering. For the RbCoFe colloid, the broad absorption band centered around 510 nm corresponds to the metal-to-metal charge transfer (MMCT) excitation. As shown by Figure S6, the absorbance of the KNiCr and KNiFe samples is negligible at 690 nm (wavelength used for the photo-crystallography experiments).

Table S3 Main characteristics of the KNiCr, KNiFe and RbCoFe samples used for the UV-vis absorption measurements

	hydrodynamic diameter from DLS (number average value, in nm)	atomic ratios from EDS	alkali ion content from electroneutrality
KNiCr	58(2)	Cr/Ni = 0.66(2)	K/Ni= 0.00(6)
KNiFe	70(2)	Fe/Ni =0.64(2)	K/Ni= 0.00(6)
RbCoFe	22(1)	Fe/Co = 0.84(1)	Rb/Co = 0.50(3)[a]

[a] value measured by EDS from the Rb L lines and Co K lines.

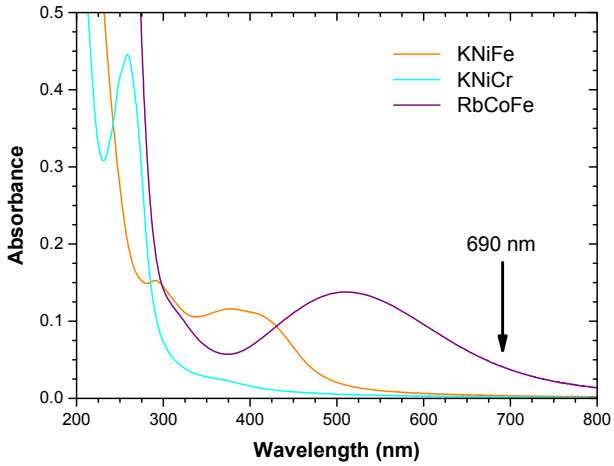

Fig. S6 UV-vis absorption spectra of colloidal solutions of RbCoFe (0.352 g/L), KNiCr (0.250 g/L) and KNiFe (0.255 g/L) for 2 mm-thick cuvettes.

Photo-crystallography experiments.

The raw 2-dimensional images were integrated using the Bubble suite[1] and were corrected for intensity fluctuations of the incident x-rays. Figure S7 shows the time-dependent PXRD patterns for the RbCoFe@KNiCr (**2**) and RbCoFe@KNiFe (**3**) samples measured under continuous irradiation. Kinetic curves of Figure 6 in the main text were obtained using the Sleuth subroutine of the SNBL Toolbox.[1,2] The integrated intensity of the peak at about 19.25° in 2θ (more precisely the area of the hatched zone) was monitored as a function of irradiation time. Curves were subsequently normalized to 100% (intensity of the peak before irradiation) and 0% (background level after irradiation).

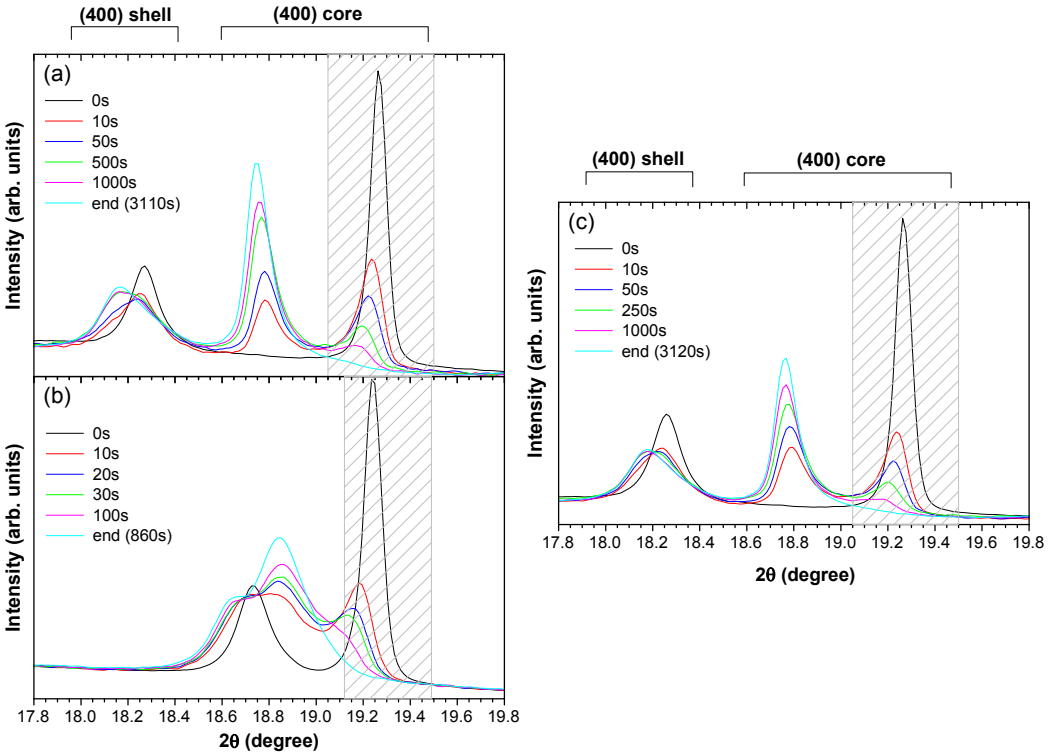

Fig. S7. Time-dependent changes of the (400) diffraction lines for the core and shell components in the two heterostructures: RbCoFe@KNiCr (a) and RbCoFe@KNiFe (b), λ= 0.8297 Å. Comparison is made with RbCoFe@RbNiCr particles (c).

1 V. Dyadkin, P. Pattison, V. Dmitriev and D.Chernyshov, J. *Synchrotron Rad.*, 2016, **23**, 825.

2 http://www.esrf.eu/home/UsersAndScience/Experiments/CRG/BM01/bm01-a/image.htm/snbl-tool-box.html.

We checked that the samples systematically decay back to the initial state, by measuring again their x-ray diffraction pattern after warming to room temperature and then fast cooling to 11 K. The reproducibility of these photo-induced structural transformations was also addressed for the RbCoFe@KNiFe sample. We found that both the time-dependent changes of the (*h*00) peaks and the final states after irradiation were comparable to the first data set shown in Figure S7(b). In addition, we measured the behavior of a RbCoFe@RbNiCr heterostructure, with a similar 11 nm shell thickness, see Figure S7(c) and Table 2. The main features of the photo-induced transition (steady states and kinetics) were found to be strictly comparable to the ones reported for the RbCoFe@KNiCr core-shell particles (**2**).

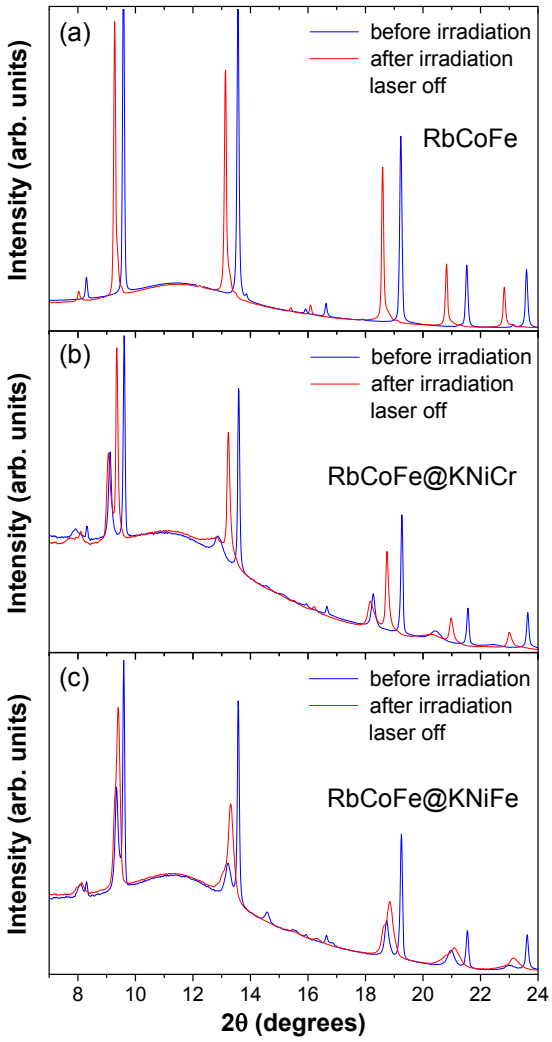

Fig. S8. PXRD patterns before and after light irradiation at 11 K for bare RbCoFe particles (a), RbCoFe@KNiCr (b) and RbCoFe@KNiFe (c) core-shell samples (λ= 0.8297 Å).

X-ray absorption spectroscopy at the Co and Fe K-edges: data reduction and fitting procedure.

At the Co K-edge, spectra were recorded using a 5 eV step between 7600 and 7700 eV, a 0.4 eV step up to 7750 eV and a 0.05 $Å^{-1}$ *k*-step for the EXAFS region (7760-8347 eV). At the Fe K-edge, data were collected over an energy range restricted to XANES, with steps of 2 eV for the pre-edge (7000-7100 eV), 0.4 eV for the main edge (7100-7140 eV) and 0.05 A^{-1} in *k* for the post-edge (7140-7270 eV) regions. Spectra relative to each element of the Canberra detector were first inspected before merging. Spectra corresponding to deteriorated elements or showing a poor signal-to-noise ratio were systematically rejected.

Spectra were corrected for pre-edge and post-edge absorption and subsequently normalized. The background was determined by a linear fit from -110 to -40 eV below the edge. The standard procedure to correct for post-edge absorption is to use a cubic spline. However, we found that the procedure implemented in the ATHENA 0.9 software package[3] is very sensitive to the

clamping points chosen for the normalization range. As we observed that the absorption at the Co K-edge exhibits oscillations around a weakly decreasing function after pre-edge correction, we chose to fit the 7820-8280 eV energy range with a linear function and normalize all XANES spectra by dividing by a constant factor determined as the value of this function at the inflection point of the absorption edge, E_0. We checked that the value of E_0, which varies from 7723 to 7726 eV for pure Co^{2+} and Co^{3+} based-samples, has virtually no influence on the maximum intensity of the white line for samples containing both Co^{2+} and Co^{3+} species (less than 0.008% change).

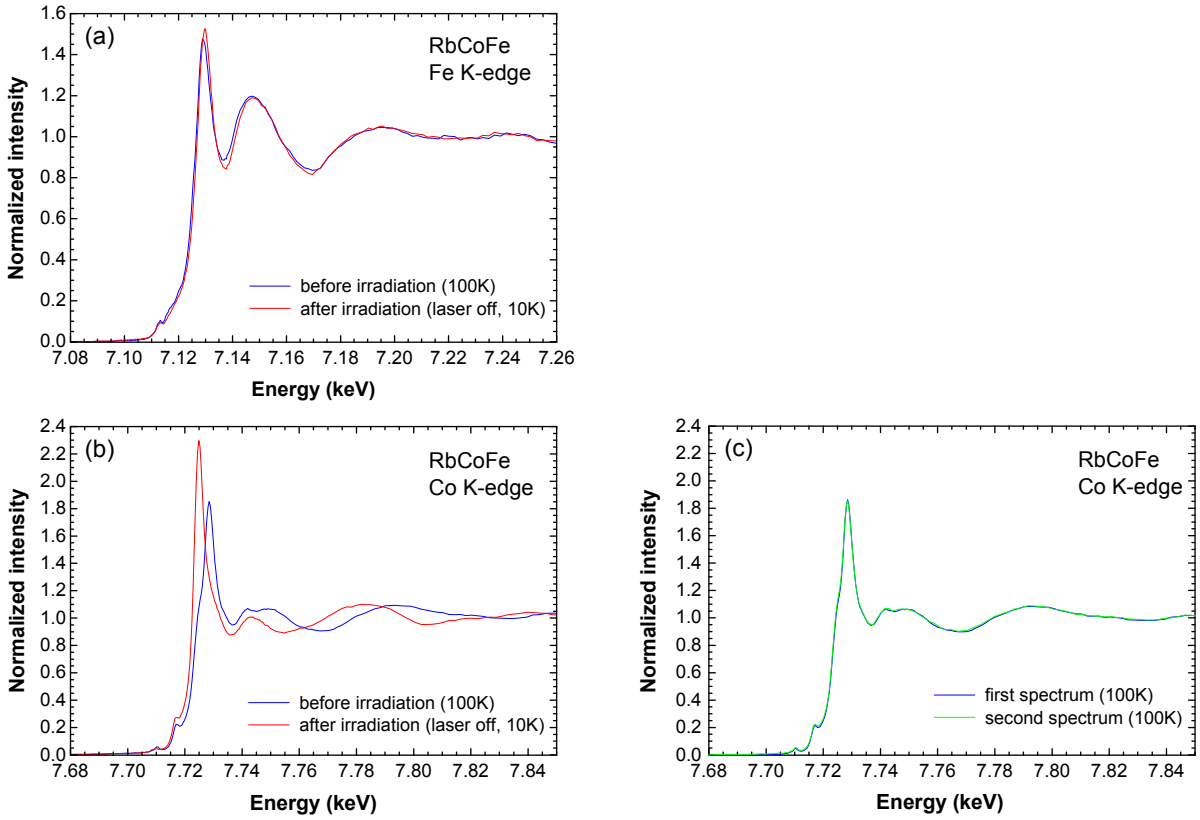

Fig. S9. XANES spectra of $Rb_{0.5}Co[Fe(CN)_6]_{0.8}$. zH_2O bare particles measured at the Fe K-edge (a) and at the Co K-edge (b). The blue curves correspond to data recorded at 100 K, with no significant photoexcitation induced by the x-ray beam, while the red curves are ascribed to data after 1 hour irradiation at 10 K using the laser diode (690 nm, ~ 2 $W.cm^{-2}$). These spectra mostly show a shift of the main line at the Fe K-edge, from 7129.1 to 7129.8 eV, associated with the $Fe^{2+} \rightarrow Fe^{3+}$ valence change. A splitting is clearly visible at the Co K-edge before irradiation, with two well resolved absorption lines, at 7725 eV for Co^{2+} ions and at 7728.5 eV for Co^{3+} ions. (c) Example of two consecutive spectra measured at 100 K at the Co K-edge to illustrate the absence of photoexcitation induced by the incident x-rays for comparison with Figure 5.

XANES spectra at the Co K-edge were fitted to the sum of two Lorentzian functions (representative of discrete $1s \rightarrow 4p$ transitions for pure Co^{2+} and Co^{3+} species) and of a single arctangent function modeling transitions to the continuum states[4]. The fit was restricted to the 7720-7732 eV energy range. To reduce the number of refined parameters, the position of the two Lorentzian functions were fixed (to average values determined from the analysis of spectra recorded during a slow photo-excitation for RbCoFe bare particles), all other parameters were let free to vary. As the main line of the Co^{3+} ions may overlap with absorption bands related to multielectronic excitations of the Co^{2+} species, the Co^{2+} fraction was finally obtained by dividing the integral of the lorentzian peak related to the Co^{2+} contribution by the one found for the $Rb_{0.5}Co[Fe(CN)_6]_{0.8}$. zH_2O bare particles after photo-excitation which is representative of 100% Co^{2+} (see Figure 5 in the main text). Note that this latter area is identical to the one found for a $Co[Fe(CN)_6]_{0.7}$. $4.6H_2O$ reference sample which contains only Co^{2+} ions and that does not display thermally or photo-induced electron transfer. Analyses were made without self-absorption corrections. Taking self-absorption into account would increase by 2% maximum the Co^{2+} fractions mentioned in the main text.

Note that the electronic changes at the Co K edge induced under laser irradiation were fully reversible after warming back the pellets up to 100 K.

---

3 B. Ravel and M. Newville, *J. Synchrotron Rad.*, 2005, **12**, 537.

4 D.C. Koningsberger and R. Prins, *X-ray absorption*. John Wiley & Sons: 1988.